Available online at www.sciencedirect.com
ScienceDirect
Biochemical and Biophysical Research Communications 361 (2007) 91–96
BBRC
www.elsevier.com/locate/ybbrc

Adsorption mechanism of BMP-7 on hydroxyapatite (001) surfaces

Hailong Zhou, Tao Wu, Xiuli Dong, Qi Wang *, Jiawei Shen

Department of Chemistry, Zhejiang University, Hangzhou 310027, PR China

Received 16 June 2007
Available online 16 July 2007

Abstract

Many properties and functions of bone-related proteins perform through the interface with the hydroxyapatite. However, the mechanism of difference of proteins adsorbing behaviors caused by the variation of calcium and phosphate ions on hydroxyapatite is still unclear at atomic level. In this work, we investigated the site-selective adhesion and the adsorption mechanism of protein BMP-7 to the hydroxyapatite surfaces in aqueous media during adsorption and desorption processes. Molecular dynamics (MD) and steered molecular dynamics (SMD) simulations combined with trajectory analysis were employed to give insight into the underlying behaviors of BMP-7 binding. The results suggest that the adsorption sites could be divided into two categories: COO^- and NH_2/NH_3^+. For COO^-, the adsorption phenomenon is driven by the electrostatic interaction formed between the negative charged carboxylate groups and the Ca1 cations on the hydroxyapatite surface. While for NH_2/NH_3^+, the interaction is through the intermolecular H-bonds between the N-containing groups and the phosphate on the hydroxyapatite surface.
© 2007 Elsevier Inc. All rights reserved.

Keywords: Bone morphogenetic proteins (BMPs); Hydroxyapatite (HAP); Interactions; Adsorption–desorption mechanism; Molecular simulation

Hydroxyapatite [HAP, $Ca_{10}(PO_4)_6(OH)_2$] is the predominant inorganic component of human bones and teeth. In the last decade, the HAP crystals have received much attention in materials science and medical fields because of its special surface interaction properties and biocompatibility [1,2]. Currently, it has been widely used in many medical practices such as bone implant materials [3]. It is found that when HAP is exposed in the organism matrix *in vivo*, its surface is rapidly covered by a proteineous layer [4]. The organic–inorganic interface plays an important role in the functions of HAP-related proteins. Moreover, the protein–HAP interaction also serves as a useful model to understand the mechanism of how crystal growth mediated by proteins in body [5]. So far, there have been many studies applied to identify the molecular mechanisms underlying protein's interaction with HAP at the inorganic mineral interface. The COO^- terminus of amelogenin is one of the closest groups to the HAP surface [6], and the loss of the charged COO^- terminal of amelogenin results in reduction of the affinity to HAP, as characterized by Moradian-Oldak [7]. The H–D (hydrogen–deuterium) exchange experiment suggested that the binding interaction between lysozyme and the HAP could be attributed to the positively charged residues of lysozyme [8]. In addition, many experimental techniques have been developed and applied to study the important protein–HAP interaction. For example, solid-state NMR (ssNMR) and atomic force microscopy (AFM) are extensively used to explore their structure features [9,10]. Recently, thermodynamic characterization is also introduced to the research of protein binding [11]. Although these techniques and methods have greatly extended our knowledge of the dynamic behavior of proteins on HAP surface in this field, it is still difficult to completely understand the adsorption process, especially the mechanism of protein adsorbing onto HAP on atomic level.

Molecular dynamics (MD) simulation has been proven to be a very useful tool to study the adsorption of proteins at the atomic level [12]. It can provide detailed information about the structural changes of effective adsorption sites.

* Corresponding author. Fax: +86 571 87951895.
E-mail address: qiwang@zju.edu.cn (Q. Wang).

0006-291X/$ - see front matter © 2007 Elsevier Inc. All rights reserved.
doi:10.1016/j.bbrc.2007.06.169

Steered molecular dynamics (SMD) can be used to explicitly illustrated adsorption and desorption characteristics [13–15]. These two techniques are essential to properly understand the adsorption behavior of protein on the inorganic materials at the atomic level. In this work, we reported the adsorption mechanism of BMP-7 on the HAP (001) surface through adsorption and desorption processes by MD and SMD simulations. BMP-7, which is one of the bone morphogenetic proteins (BMPs), contains 112 residues. And it plays a key role in the formation of bones. As reported, this protein may influence skeletal development and growth in children [16]. Therefore, the detailed investigation of interaction between the protein BMP-7 and HAP is of great biological and medical significance.

There are many factors contributing to the interaction between the HAP and BMP-7, such as different protein orientations and different Ca/P ratios. However, it is out of the capability of current techniques to take all the factors into account simultaneously. Experimental studies have suggested that the variation of calcium and phosphate ions on the crystal surfaces play an important role in the adsorption of proteins onto HAP [17]. Therefore, we mainly studied the influence of different Ca/P ratios. Typically, two extreme HAP modules (Systems I and II) were obtained through 'cutting' the HAP crystal structure perpendicular to the [001] direction [18]. System I represents the surface sliced only including the Ca1 cations, while System II represents the surface sliced including Ca2 and phosphate ions, as shown in Fig. 1.

Simulation details

The initial structure of BMP-7 was taken from the protein data bank (PDB Accession No. 1M4U). The original module of HAP ($P6_3/m$) was extracted from the American Mineralogist Crystal Structure Database [19] and its unit-cell parameters are $a = b = 0.943$ nm and $c = 0.688$ nm.

In order to obtain the optimized geometry of BMP-7, an energy minimization was firstly performed, and a 1 ns MD relaxation in water media (with normal density, SPC model [20]) was followed. Then two simulation systems, which were composed of the optimized BMP-7 module, HAP module and water molecules (by putting the BMP-7 onto the HAP and then adding water), were built up to study the interactions between the BMP-7 and HAP. Both of the two extreme hexagonal HAP modules contain $9 \times 7 \times 6$ unit-cells ($\sim 84.8 \times 66.0 \times 41.3$ Å^3). The HAP module (16,632 atoms) and the BMP-7 molecule (1741 atoms) were immerged in a periodic water box, in which SPC model water molecules were employed. Two sodium ions were added to neutralize the system, which is especially necessary since the BMP-7 protein carries two negative charges. The volume of each water box was $84.9 \times 57.2 \times 115.6$ Å^3. There were 50,736 atoms for System I and 50,688 atoms for System II (water density is approximately 1.0 g cm^{-3}), respectively.

All simulations were performed with NAMD [21] using Charmm27 force field [22] with the hydroxyapatite parameters supplemented. Periodic boundary conditions were applied in all directions. The Particle-mesh Ewald summation was employed to calculate the long-ranged electrostatic interactions, with a cutoff distance of 12 Å for the separation of the direct and reciprocal space. The van der Waals interactions were truncated at 12 Å. The force field parameters for HAP were taken from the work of Hauptmann [23]. The simulations were carried out with a time step of 2 fs in the NpT ensemble. A constant temperature of 310 K and constant pressure of 101.3 kPa were managed in the simulations with the Langevin method.

SMD is a novel approach to study the dynamics of binding–unbinding events in the biomolecular systems and of their elastic properties. The constant velocity pulling (PCV) is one of the basic techniques of SMD. In PCV simulation, the SMD atom is attached to a dummy atom via a virtual spring. This dummy atom moved at a constant velocity and then the force between them is measured using:

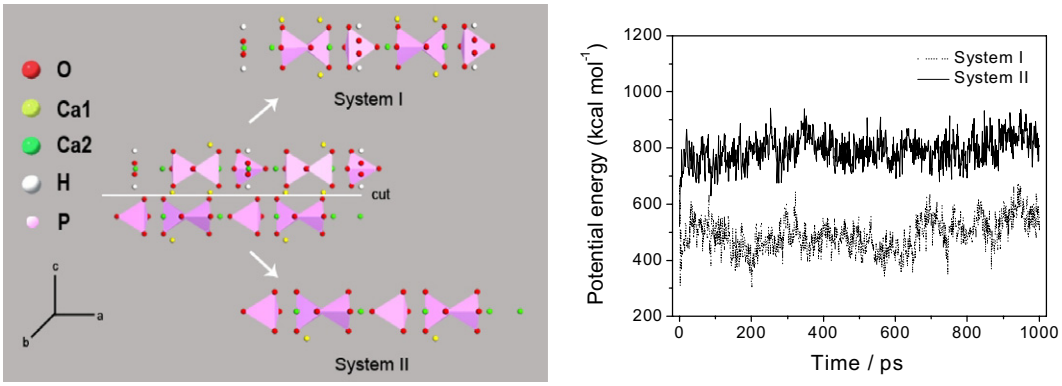

Fig. 1. (Left) Systems of the HAP (001) surface investigated. The upper system (denoted as System I) represents the surface sliced to include all the Ca1 cations in the outermost layer, and the bottom system (System II) represents the surface sliced to include the Ca2 and phosphate ions in the outermost layer. (Right) Potential energy of the protein BMP-7 with respect to MD simulation time. A relatively small fluctuation for both surfaces, Systems I and II, which suggests the equilibrium was achieved.

$$\vec{F} = -\nabla U \quad (1)$$

$$U = \frac{1}{2}k[vt - (\vec{r} - \vec{r}_0) \cdot \vec{n}]^2 \quad (2)$$

where U is the potential energy, k is the spring constant, v stands for the pulling velocity, t means the time, $\vec{n}$ is the direction of pulling, $\vec{r}$ and $\vec{r}_0$ is the instantaneous position and the initial position of the SMD atoms, respectively [24].

To obtain the reasonable parameters of PCV in this work, a series of simulations with varied parameters were performed and the results were checked carefully in order to get a converged one. Once Systems I and II were built up, we followed a three-step strategy: (i) first, we carried out direct PCV simulation ($k = 2$ kcal mol^{-1} Å^{-2}, $v = 0.25$ Å ps^{-1}) of the BMP-7 module close to the HAP surface for each system. The external force was applied along the *c*-axis of HAP and towards the HAP surface. This PCV process accelerated the adsorption process of BMP-7 onto the HAP surfaces; (ii) then, in both of the two systems, we conducted an equilibrium MD simulation of 1 ns in search of the most stable state of BMP-7 adsorbed without any external force; (iii) third, based on the equilibrium structure, we conducted desorption PCV simulations to study the desorption details. For System I, the spring constant was set to be 100 kcal mol^{-1} Å^{-2}, and the pulling velocity was 0.65 Å ps^{-1}. For System II, they were 100 kcal mol^{-1} Å^{-2} and 0.25 Å ps^{-1}, respectively. The snapshots of PCV could be intercepted from the trajectories by the molecular graphics package VMD [25].

Results and discussion

Equilibrium adsorption

The MD simulation is essential to achieve an equilibrium state, and generally the potential energy of biomolecule was used to judge whether the system achieves equilibrium or not. To describe the adsorption states, the potential energy of biomolecule was extracted individually from the simulation systems [12,26]. It was defined as $E_{pot} = E_{tot} - E_{kin}$, where E_{pot} is the potential energy, E_{tot} is the total energy, and E_{kin} is the kinetic energy of the protein. Fig. 1 illustrates the potential energy of BMP-7 with respect to MD simulation time for both systems (Systems I and II). One could notice that the energy curves of both systems fluctuate slightly after 700 ps. It indicates that only minor local change may occur for the protein during the last 300 ps. The results of MD simulation show that the systems have reached steady adsorption states, and the time of 1 ns is long enough for BMP-7 to relax and adsorb onto the HAP surface. There is a difference in potential energy for Systems I and II, this phenomenon provides a strong basis for future BMP-7 potential energy-adsorption studies. The *z*-coordinates of adsorption groups also show that these two systems have reached equilibration (Fig. 2). The distance between these adsorption groups and the HAP surface keeps less than 5 Å, which means the protein BMP-7 adsorbed on the HAP surface steadily (conventionally, 5 Å is taken as the upper limit being adsorbed for the contact distance to the surface [12]). During 1 ns MD simulation, the adsorption groups in both systems grasp the HAP surface like claws, while the remaining parts are dynamic in aqueous media.

Desorption from two category interfaces (Systems I and II)

After 1 ns MD simulation, without any disturbances applied to the BMP-7 and HAP, an equilibrium state was relegated to the PCV (SMD) simulation as the starting state. A PCV simulation was conducted to make the protein BMP-7 apart from the HAP surface along the *c*-axis of HAP. During PCV simulation, all the atoms of HAP crystal were fixed and an external force was applied uniformly to every atom in the backbone of BMP-7 to keep BMP-7 moving at a constant velocity. As to the water molecules, they all moved freely under periodic boundary conditions. The force changes with respect to time were recorded through the PCV simulation.

System I

For System I, we observed that the adsorption occurs at the COO^- group. The driving force comes mainly from the electrostatic attraction presented between the adsorption groups and the Ca1 cations on the HAP surface. When an external force exists, the adsorption groups will be mainly influenced by two types of forces: the electrostatic force mentioned above and the external force we applied. If the external force exceeds the other one, the residue would begin to be desorbed from the HAP surface, as shown in Fig. 3A. At the beginning of PCV simulation, the protein BMP-7 distorts in order to maintain its structural integrity and to resist against the external force. With the disturbance, the BMP-7 was compelled to deform and many weak intramolecular interactions were broken down. This is why there is a sharp climbing peak 8638 pN at 7.2 ps, as shown in Fig. 3C. With the time passing by, the external force applied to BMP-7 makes the COO^- group of Glu42 (a_1) break away from the HAP surface. This is corresponding to the second peak in Fig. 3C. The time is 14.2 ps, and the force is 5517 pN. The *z*-coordinate (distance to the HAP surface) of the C atom of COO^- [Glu42 (a_1)] apparently illustrates this desorption process. At the beginning, this group keeps less than 5 Å from the HAP surface. While, from 14.2 ps, the distance increases sharply, this indicates that the COO^- [Glu42 (a_1)] begins to be desorbed from the HAP surface. At 19.2 ps, there is a peak 3523 pN in Fig. 3C, which is because of the desorption of the COO^- [Asp119 (a_2)], also as shown in Fig. 3A. Similarly, the desorption of the COO^- [Glu60 (a_3)] results in the peak of 4859 pN at 26.2 ps. The COO^- [Asp54 (a_4)] escapes from the surface of HAP, thus a

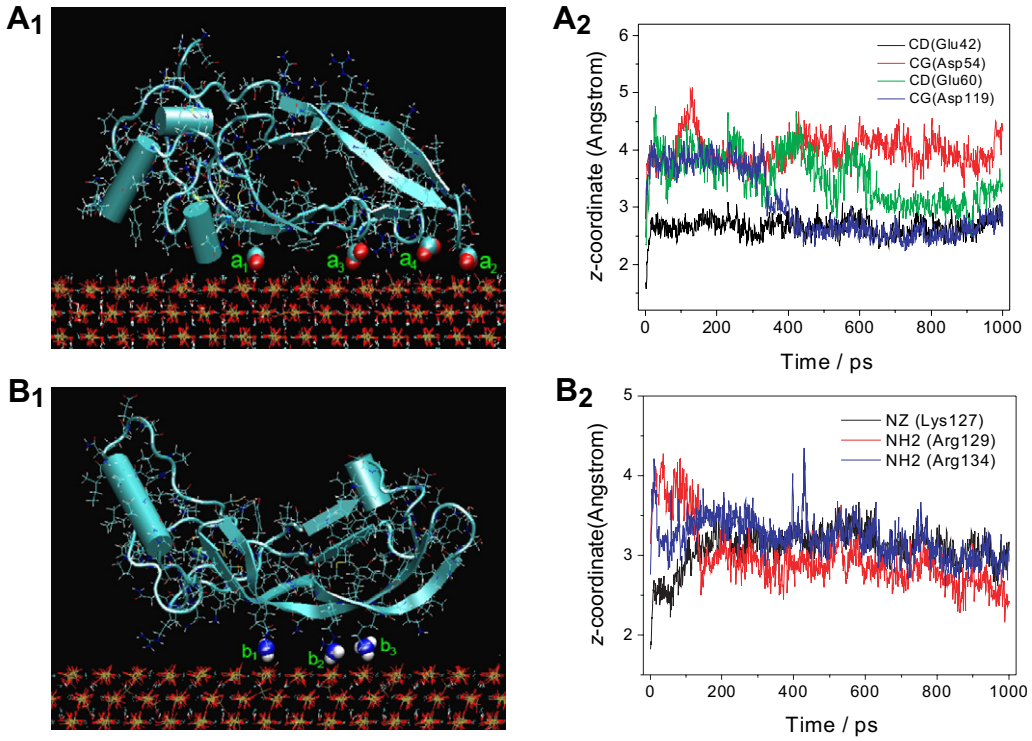

Fig. 2. (Left) BMP-7 adsorbed on the HAP (001) surfaces after 1 ns MD runs, the labeled residues are the adsorption sites of BMP-7. (A_1) on System I, the charged carboxylate groups of Glu42 (a_1), Asp119 (a_2), Glu60 (a_3) and Asp54 (a_4), and (B_1) on System II, the amido functional groups of Arg134 (b_1), Arg129 (b_2) and Lys127 (b_3). (Right) Distances (*z*-coordinates) between the adsorbed atoms of protein BMP-7 to the HAP (001) surface in the *c*-axis with respect to MD run time. (A_2) on System I, and (B_2) on System II.

corresponding peak of 3495 pN is observed at 33.6 ps. Fig. 3B illustrates the interaction energy between BMP-7 and the HAP surface during the PCV simulation. These groups are able to resist the disturbance during the whole simulation, which indicates a strong interaction between them. It should be pointed out that the carboxylate groups could be adsorbed on HAP firmly, but it does not mean that every carboxylate group could be adsorbed effectively [15], and the desorption sequence does not only depend on the distance of the adsorption groups to the HAP surface. In other words, the location of the carboxylate groups is an important factor. It is easy to notice that there are many small peaks in the force–time curve. They may be caused by the disturbance of water molecules during the moving of BMP-7.

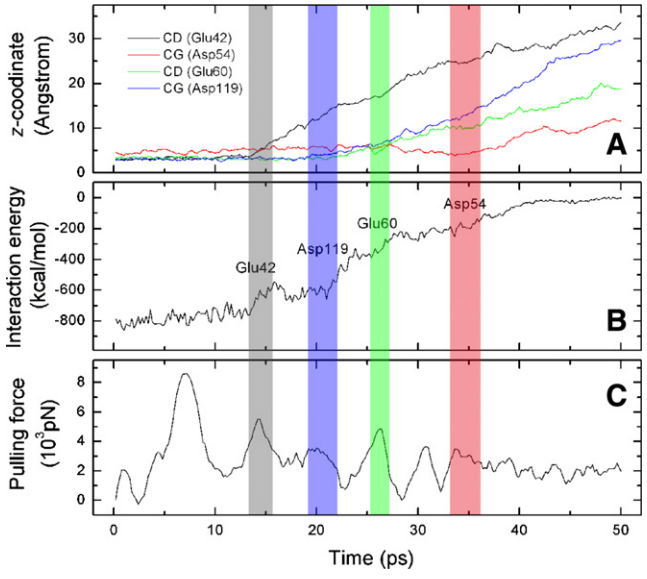

Fig. 3. (A) Distances (*z*-coordinates) between the adsorbed carboxylate atoms of protein BMP-7 to the HAP (001) surface in the *c*-axis with respect to PCV time. (B) Interaction energy between BMP-7 and the HAP surface with respect to PCV simulation time. (C) Pulling forces with respect to PCV time, starting from the MD equilibrium configuration of the System I. The virtual spring between the dummy atoms and the SMD atoms has a spring constant of 100 kcal mol^{-1} $Å^{-2}$, and the protein BMP-7 was pulled at 0.65 Å ps^{-1} using a time step of 2 fs.

System II

Comparing with the System I, the adsorption group in this system is NH_2/NH_3^+. Fig. 4C shows the plots of the external force as a function of PCV time for System II. There is a sharp force peak 6374 pN presented at 7.4 ps. This peak is caused by not only the deformation of BMP-7, but also the breaking down of the intermolecular H-bonds, which formed between NH_2 group in Arg134 (b_1) and the oxygen atom of PO_4^{3-} on the HAP surface (Fig. 4A). Generally, the H-bond should be in the form of X–H···Y, and the following three conditions should be simultaneously fulfilled [27,28]. (1) The distance between H···Y is less than 2.45 Å; (2) The distance between X···Y is shorter than 3.6 Å; and (3) The bond angle between

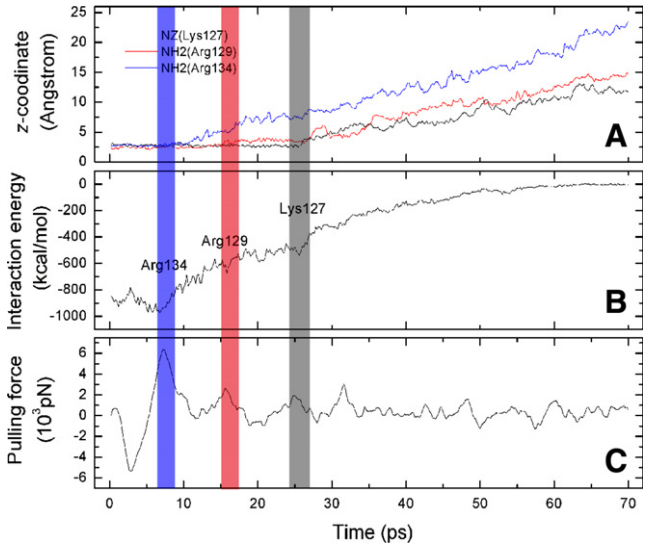

Fig. 4. (A) Distances (z-coordinates) between the adsorbed amido atoms of protein BMP-7 to the HAP (001) surface in the c-axis with respect to PCV time. (B) Interaction energy between BMP-7 and the HAP surface with respect to PCV simulation time. (C) Pulling forces with respect to PCV time, starting from the MD equilibrium configuration of the System II. The virtual spring between the dummy atoms and the SMD atoms has a spring constant of 100 kcal mol^{-1} $Å^{-2}$, and the protein BMP-7 was pulled at 0.25 Å ps^{-1} using a time step of 2 fs.

X–H and H···Y directions, θ, must be larger than 150°. For the H-bond between the NH_2 [Arg134 (b_1)] and the PO_4^{3-}, the distance of H···O is 1.665 Å, and the distance between N···O is 2.603 Å. The bond angle θ is about 156°. Similarly, at 15.6 ps, the intermolecular H-bond between NH_2 [Arg129 (b_2)] and the O atom of PO_4^{3-} is broken down (Fig. 4A), which corresponds to the force peak 2637 pN (Fig. 4C). And at 24.8 ps, with a force peak 1944 pN (Fig. 4C), the intermolecular H-bond of NH_3^+ in Lys127 (b_3) is broken down (Fig. 4A). We noticed that this group (NH_3^+) is the last one to be desorbed from the HAP surface. This is because there are three H atoms connected to the N atom with different orientations, and these three H atoms could form H-bond alternately. Therefore, the adsorption time of Lys127 (b_3) is much longer than that of NH_2 group discussed above. And it prolongs the desorption time of this group. Similarly, Fig. 4B illustrates the interaction energy between BMP-7 and the HAP surface during the PCV simulation. There is a sharp declining force peak before 3.2 ps in Fig. 4C. The reasons for this abnormal peak are not yet clarified.

Comparison of carboxylate and amido adsorption sites

On the basis of this comparative study, it was suggested that the adsorption mechanism of BMP-7 onto the HAP surface is largely related to the Ca/P molar ratios of the surface. System I is rich in positive charged Ca1 cations. The adsorption originates from the electrostatic attractive force between the binding groups of charged carboxylate in BMP-7 and these Ca1 cations. System II is lack of Ca1 cations on the HAP surface. The adsorption is caused by the intermolecular H-bonds between the adsorption groups and the phosphate on the HAP surface. Figs. 3 and 4C illustrate that the adsorptive force of System I is generally larger than that of System II, because the electrostatic force is strong interaction while H-bond is relatively weak one. So it is feasible to design and modify the adsorption materials according to the special configurations of the proteins, and it is expected that the proteins will be selectively adsorbed and separated based on the corresponding adsorption mechanism.

We would like to point out that during the process of protein adsorbing/desorbing on the HAP surface, the pH value might be one of the sensitive factors. The surface charge of protein could be adjusted with the pH value of aqueous solution, which leads to the transformation between COO^-/COOH or NH_2/NH_3^+ in proteins.

Conclusion

The adsorption sites and the adsorption mechanism of BMP-7 (one of the bone morphogenetic proteins, BMPs) onto the hydroxyapatite (HAP) surfaces were investigated from atomic level. It is reported that the Ca/P ratios on the HAP surface have great contribution to the adsorption of proteins onto the HAP. In this work, two extreme HAP surfaces were discussed. System I represents the surface sliced only including the Ca1 cations, while System II represents the surface sliced including Ca2 and phosphate ions. It is found that the adsorption sites might be divided into two categories: COO^- and NH_2/NH_3^+. Both of them play an important role in the adsorption of BMP-7 on the HAP surfaces. However, their adsorption mechanisms are greatly different. For COO^-, the adsorptive interaction is the electrostatic attractive force presented between the carboxylate group and Ca1 cations on the HAP surface. But for NH_2/NH_3^+, the major adsorptive interaction is the intermolecular H-bonds between the N-containing group and the phosphate on the HAP surface. These adsorption details may provide helpful insights to biomaterials science and medical fields, such as biomineralization, bone formation and growth, separation and purification of proteins, and implant drug device.

Acknowledgment

This work was financially supported by the National Natural Science Foundation of China (Grant Nos. 60533050 and 20576112).

References

[1] S.R. Kim, J.H. Lee, Y.T. Kim, D.H. Riu, S.J. Jung, Y.J. Lee, S.C. Chung, Y.H. Kim, Synthesis of Si, Mg substituted hydroxyapatites and their sintering behaviors, Biomaterials 24 (2003) 1389–1398.

[2] A. Barroug, M.J. Glimcher, Hydroxyapatite crystals as a local delivery system for cisplatin: adsorption and release of cisplatin in vitro, J. Orthop. Res. 20 (2002) 274–280.

[3] A. Matsuda, T. Furuzono, D. Walsh, A. Kishida, J. Tanaka, Surface modification of a porous hydroxyapatite to promote bonded polymer coatings, J. Mater. Sci. Mater. Med. 14 (2003) 973–978.
[4] K. Kandori, N. Horigami, H. Kobayashi, A. Yasukawa, T. Ishikawa, Adsorption of lysozyme onto various synthetic hydroxyapatites, J. Colloid Interf. Sci. 191 (1997) 498–502.
[5] M.L. Wallwork, J. Kirkham, J. Zhang, D.A. Smith, S.J. Brookes, R.C. Shore, S.R. Wood, O. Ryu, C. Robinson, Binding of matrix proteins to developing enamel crystals: an atomic force microscopy study, Langmuir 17 (2001) 2508–2513.
[6] W.J. Shaw, A.A. Campbell, M.L. Paine, M.L. Snead, The COOH terminus of the amelogenin, LRAP, is oriented next to the hydroxyapatite surface, J. Biol. Chem. 279 (2004) 40263–40266.
[7] J. Moradian-Oldak, N. Bouropoulos, L. Wang, N. Gharakhanian, Analysis of self-assembly and apatite binding properties of amelogenin proteins lacking the hydrophilic C-terminal, Matrix Biol. 21 (2002) 197–205.
[8] T. Aizawa, N. Koganesawa, A. Kamakura, K. Masaki, A. Matsuura, H. Nagadome, Y. Terada, K. Kawano, K. Nitta, Adsorption of human lysozyme onto hydroxyapatite: identification of its adsorbing site using site-directed mutagenesis, FEBS Lett. 422 (1998) 175–178.
[9] K. Sato, Y. Suetsugu, J. Tanaka, S. Ina, H. Monma, The surface structure of hydroxyapatite single crystal and the accumulation of arachidic acid, J. Colloid Interf. Sci. 224 (2000) 23–27.
[10] J.M. Gibson, V. Raghunathan, J.M. Popham, P.S. Stayton, G.P. Drobny, A REDOR NMR study of a phosphorylated statherin fragment bound to hydroxyapatite crystals, J. Am. Chem. Soc. 127 (2005) 9350–9351.
[11] R. Goobes, G. Goobes, C.T. Campbell, P.S. Stayton, Thermodynamics of statherin adsorption onto hydroxyapatite, Biochemistry 45 (2006) 5576–5586.
[12] G. Raffaini, F. Ganazzoli, Molecular dynamics simulation of the adsorption of a fibronectin module on a graphite surface, Langmuir 20 (2004) 3371–3378.
[13] H. Lu, K. Schulten, The key event in force-induced unfolding of Titin's immunoglobulin domains, Biophys. J. 79 (2000) 51–65.
[14] X. Dong, Q. Wang, T. Wu, H. Pan, Understanding the adsorption-desorption dynamics of BMP-2 on hydroxyapatite (001) surface, Biophys. J. 93 (2007) 750–759.
[15] X. Chen, Q. Wang, J. Shen, H. Pan, T. Wu, Adsorption of LRAP on hydroxyapatite (001) surface through $-COO^-$ claws, J. Phys. Chem. C 111 (2007) 1284–1290.
[16] A.H. Reddi, Bone morphogenetic proteins and skeletal development: the kidney–bone connection, Pediatr. Nephrol. 14 (2000) 598–601.
[17] K. Kandori, A. Fudo, T. Ishikawa, Study on the particle texture dependence of protein adsorption by using synthetic micrometer-sized calcium hydroxyapatite particles, Colloids Surf. B: Biointerfaces 24 (2002) 145–153.
[18] D. Zahn, O. Hochrein, Computational study of interfaces between hydroxyapatite and water, Phys. Chem. Chem. Phys. 5 (2003) 4004–4007.
[19] R.M. Wilson, J.C. Elliott, S.E.P. Dowker, Rietveld refinement of the crystallographic structure of human dental enamel apatites, Am. Miner. 84 (1999) 1406–1414.
[20] H.J.C. Berendsen, J.P.M. Postma, W.F. van Gunsteren, J. Hermans, Intermolecular models for water in relation to protein hydration, in: B. Pullman (Ed.), Intermolecular Forces, Reidel, Dordrecht, the Netherlands, 1981, pp. 331–342.
[21] L. Kalé, R. Skeel, M. Bhandarkar, R. Brunner, A. Gursoy, N. Krawetz, J. Phillips, A. Shinozaki, K. Varadarajan, K. Schulten, NAMD2: greater scalability for parallel molecular dynamics, J. Comp. Phys. 151 (1999) 283–312.
[22] A.D. MacKerell, D. Bashford, M. Bellott, R.L. Dunbrack, J.D. Evanseck, M.J. Field, S. Fischer, J. Gao, H. Guo, S. Ha, D. Joseph-McCarthy, L. Kuchnir, K. Kuczera, F.T.K. Lau, C. Mattos, S. Michnick, T. Ngo, D.T. Nguyen, B. Prodhom, W.E. Reiher, B. Roux, M. Schlenkrich, J.C. Smith, R. Stote, J. Straub, M. Watanabe, J. Wiórkiewicz-Kuczera, D. Yin, M. Karplus, All-atom empirical potential for molecular modeling and dynamics studies of proteins, J. Phys. Chem. B 102 (1998) 3586–3616.
[23] S. Hauptmann, H. Dufner, J. Brickmann, S.M. Kast, R.S. Berry, Potential energy function for apatites, Phys. Chem. Chem. Phys. 5 (2003) 635–639.
[24] B. Isralewitz, J. Baudry, J. Gullingsrud, D. Kosztin, K. Schulten, Steered molecular dynamics investigations of protein function, J. Mol. Graph. Model. 19 (2001) 13–25.
[25] W. Humphrey, A. Dalke, K. Schulten, VMD: visual molecular dynamics, J. Mol. Graph. 14 (1996) 33–38.
[26] G. Raffaini, F. Ganazzoli, Simulation study of the interaction of some Albumin subdomains with a flat graphite surface, Langmuir 19 (2003) 3403–3412.
[27] W.L. Jorgensen, Structure and properties of liquid methanol, J. Am. Chem. Soc. 102 (1980) 543–549.
[28] W.L. Jorgensen, M. Ibrahim, Pressure dependence of hydrogen bonding in liquid methanol, J. Am. Chem. Soc. 104 (1982) 373–378.